# Polarization operator contributions to the Lamb shift and hyperfine splitting

Michael I. Eides*
*Department of Physics and Astronomy, University of Kentucky, Lexington, Kentucky 40506, USA*
*and Petersburg Nuclear Physics Institute, Gatchina, St. Petersburg 188300, Russia*

Valery A. Shelyuto†
*D. I. Mendeleev Institute of Metrology, St. Petersburg 198005, Russia*
(Received 19 May 2003; published 9 October 2003)

We calculate radiative corrections to the Lamb shift of order $\alpha^3(Z\alpha)^5 m$ and radiative corrections to hyperfine splitting of order $\alpha^3(Z\alpha)E_F$ generated by the diagrams with insertions of radiative photons and electron polarization loops in the graphs with two external photons. We also obtain the radiative-recoil correction to hyperfine splitting in muonium generated by the diagrams with the $\tau$ polarization loop.

DOI: 10.1103/PhysRevA.68.042106 PACS number(s): 12.20.Ds, 31.30.Jv, 32.10.Fn, 36.10.Dr

## I. INTRODUCTION

Nonrecoil corrections of order $\alpha^3(Z\alpha)^5 m$ to the Lamb shift and corrections of order $\alpha^3(Z\alpha)E_F$ to hyperfine splitting are generated by three-loop radiative insertions in the skeleton diagram in Fig. 1. Respective corrections of lower orders in $\alpha$ generated by one- and two-loop radiative insertions are already well known (see, e.g., Ref. [1]). The crucial observation, which greatly facilitates further calculations, is that the scattering approximation is adequate for calculation of all corrections of order $\alpha^n(Z\alpha)^5 m$ and $\alpha^n(Z\alpha)E_F$ (see, e.g., a detailed proof in Ref. [2]). One may easily understand the physical reasons which lead to this conclusion. Consider the matrix elements of the skeleton diagram in Fig. 1 with the on shell external electron lines calculated between the free-electron spinors, and multiplied by the square of the Schrödinger-Coulomb wave function at the origin. They are described by the infrared divergent integral

$$-\frac{16(Z\alpha)^5}{\pi n^3}\left(\frac{m_r}{m}\right)^3 m\int_0^\infty \frac{dk}{k^4}\,\delta_{l0} \tag{1}$$

in the case of the Lamb shift, and by the infrared divergent integral

$$\frac{8Z\alpha}{\pi n^3}E_F\int_0^\infty \frac{dk}{k^2} \tag{2}$$

in the case of hyperfine splitting. In these integrals $k$ is the dimensionless momentum of the exchanged photons measured in the units of the electron mass. We define the Fermi energy $E_F$ as

$$E_F=\frac{16}{3}Z^4\alpha^2\frac{m}{M}(1+a_\mu)\left(\frac{m_r}{m}\right)^3 chR_\infty, \tag{3}$$

where $m$ is the electron mass, $M$ is the muon mass, $m_r$ is the reduced mass, $\alpha$ is the fine structure constant, $c$ is the velocity of light, $h$ is the Planck constant, $R_\infty$ is the Rydberg constant, $a_\mu$ is the muon anomalous magnetic moment, and $Z$ is the nucleus charge in terms of the electron charge ($Z=1$ for hydrogen and muonium).

Let us consider radiative insertions in the skeleton two-photon diagram in Fig. 1. Account of these corrections effectively leads to insertion of an additional factor $L(k)$ in the divergent integrals above, and while this factor has at most a logarithmic asymptotic behavior at large momenta and does not spoil the ultraviolet convergence of the integrals, in the low-momentum region it behaves as $L(k)\sim k^2$ (again up to logarithmic factors), and improves the low-frequency behavior of the integrand. However, the integral for the Lamb shift is sometimes still divergent after inclusion of the radiative corrections because the two-photon-exchange diagram, even with radiative corrections, contains a contribution of the previous order in $Z\alpha$. This spurious contribution should be removed by subtracting the leading low-momentum term from $L(k)/k^4$. The result of such subtraction is a convergent integral, where the low integration momenta (of atomic order $mZ\alpha$) in the exchange loops are suppressed, and the effective loop integration momenta are of order $m$. Then it is clear that small virtuality of the external electron lines would lead to an additional suppression of the matrix element under consideration, and it is sufficient to consider the diagrams only with on-mass-shell external momenta for calculation of the contributions to the energy shifts. As an additional bonus of this approach one does not need to worry about the ultraviolet divergence of the one-loop radiative corrections. The subtraction automatically eliminates any ultraviolet divergent terms and the result is both ultraviolet and infrared finite.

Below we consider contributions to the Lamb shift and hyperfine splitting generated by radiative insertions in the skeleton diagram in Fig. 1. We also obtain radiative-recoil correction to hyperfine splitting generated by the $\tau$ polarization loop.

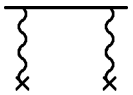

FIG. 1. Skeleton two-photon diagram.

*Email addresses: eides@pa.uky.edu, eides@thd.pnpi.spb.ru
†Email address: shelyuto@vniim.ru

 

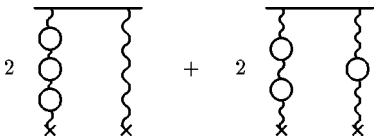

FIG. 2. Three one-loop polarizations.

## II. CORRECTIONS OF ORDER $\alpha^3(Z\alpha)^5 m$ TO LAMB SHIFT AND OF ORDER $\alpha^3(Z\alpha)E_F$ TO HYPERFINE SPLITTING

### A. Diagrams with three one-loop electron vacuum polarizations

#### *1. Lamb shift*

Each polarization loop in the diagrams in Fig. 2 corresponds to insertion of the vacuum polarization operator $(\alpha/\pi)k^2 I_{1e}$ in the Lamb shift skeleton integral in Eq. (1), where

$$I_{1e}=\int_0^1 dv\,\frac{v^2(1-v^2/3)}{4+k^2(1-v^2)}. \tag{4}$$

Inserting also the multiplicity factor 4, we obtain an analytic expression for the contribution to the Lamb shift generated by the diagrams in Fig. 2 in the form

$$\delta E_L^{(1)}=-\frac{64\alpha^3(Z\alpha)^5}{\pi^4 n^3}\left(\frac{m_r}{m}\right)^3 m\int_0^\infty dk k^2 I_{1e}^3. \tag{5}$$

Calculating the integral numerically we obtain

$$\delta E_L^{(1)}=-0.021\,458(1)\,\frac{\alpha^3(Z\alpha)^5}{\pi^2 n^3}\left(\frac{m_r}{m}\right)^3 m \tag{6}$$

or

$$\delta E_L^{(1)}=-0.002\,16\ \ \mathrm{kHz} \tag{7}$$

for the $1S$ level in hydrogen.

#### *2. Hyperfine splitting*

We obtain the expression for the radiative correction to hyperfine splitting generated by the diagrams in Fig. 2 by inserting the polarization loops in the skeleton integral in Eq. (2),

$$\delta E_{HFS}^{(1)}=\frac{32\alpha^3(Z\alpha)}{\pi^4 n^3}E_F\int_0^\infty dk k^4 I_{1e}^3. \tag{8}$$

After numerical calculations we have

$$\delta E_{HFS}^{(1)}=2.568\,3(4)\frac{\alpha^3(Z\alpha)}{\pi^2}E_F \tag{9}$$

or

$$\delta E_{HFS}^{(1)}=0.003\,29\ \ \mathrm{kHz} \tag{10}$$

for the ground state in muonium.

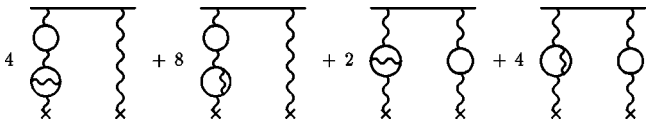

FIG. 3. One- and two-loop polarizations.

### B. Diagrams with two-loop and one-loop electron vacuum polarizations

#### *1. Lamb shift*

The integral for the diagrams in Fig. 3 is obtained from the skeleton integral in Eq. (1) by insertion of the one-loop vacuum polarization $(\alpha/\pi)k^2 I_{1e}$, and the two-loop vacuum polarization $(\alpha/\pi)^2 k^2 I_{2e}$ (see, e.g., Refs. [3,4])

$$\begin{aligned}I_{2e}=\frac{2}{3}\int_0^1\frac{v\,dv}{4+k^2(1-v^2)}\Bigg\{&(3-v^2)(1+v^2)\left[\mathrm{Li}_2\left(-\frac{1-v}{1+v}\right)\right.\\&\left.+2\ \ \mathrm{Li}_2\left(\frac{1-v}{1+v}\right)+\frac{3}{2}\ln\frac{1+v}{1-v}\ln\frac{1+v}{2}-\ln\frac{1+v}{1-v}\ln v\right]\\&+\left[\frac{11}{16}(3-v^2)(1+v^2)+\frac{v^4}{4}\right]\ln\frac{1+v}{1-v}\\&+\left[\frac{3}{2}v(3-v^2)\ln\frac{1-v^2}{4}-2v(3-v^2)\ln v\right]\\&+\frac{3}{8}v(5-3v^2)\Bigg\},\end{aligned} \tag{11}$$

where the dilogarithm $\mathrm{Li}_2(x)$ is defined as $\mathrm{Li}_2(z)=-\int_0^z dt\,\ln(1-t)/t$.

Inserting in the skeleton integral in Eq. (1) also the multiplicity factor 6, we obtain an analytic expression for the contribution to the Lamb shift generated by the diagrams with the one- and two-loop polarization blocks in Fig. 3,

$$\delta E_L^{(2)}=-\frac{96\alpha^3(Z\alpha)^5}{\pi^4 n^3}\left(\frac{m_r}{m}\right)^3 m\int_0^\infty dk I_{1e}I_{2e}. \tag{12}$$

After numerical calculations we obtain

$$\delta E_L^{(2)}=-0.390\,152(7)\,\frac{\alpha^3(Z\alpha)^5}{\pi^2 n^3}\left(\frac{m_r}{m}\right)^3 m \tag{13}$$

or

$$\delta E_L^{(2)}=-0.039\,21\ \ \mathrm{kHz} \tag{14}$$

for the $1S$ level in hydrogen.

#### *2. Hyperfine splitting*

In the case of hyperfine splitting we obtain the expression for the energy shift generated by the diagrams in Fig. 3 with the help of the skeleton integral in Eq. (2),

$$\delta E_{HFS}^{(2)}=\frac{48\alpha^3(Z\alpha)}{\pi^4 n^3}E_F\int_0^\infty dk k^2 I_{1e}I_{2e}. \tag{15}$$

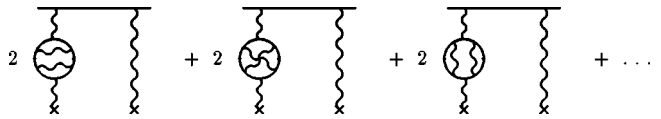

FIG. 4. Three-loop polarizations.

After numerical calculations we have

$$\delta E^{(2)}_{HFS}=3.559\,9(2)\frac{\alpha^3(Z\alpha)}{\pi^2}E_F \tag{16}$$

or

$$\delta E^{(2)}_{HFS}=0.004\,56\ \ \mathrm{kHz} \tag{17}$$

for the ground state in muonium.

### C. Diagrams with three-loop electron vacuum polarization

#### *1. Lamb shift*

For calculation of the correction generated by the diagrams in Fig. 4 we need the three-loop vacuum polarization operator $(\alpha/\pi)^3k^2I_{3e}$. This operator in QED and QCD was considered in a series of papers [5–9]. As a result, eight leading terms in the low- and seven in the high-momentum asymptotic expansions in the powers of the momentum were calculated analytically. Some of the coefficients were presented in Refs. [7,9] only in the $\widetilde{MS}$ scheme and only for the case of QCD. We adjusted these results for the case of the momentum renormalization scheme used in QED, and constructed an interpolation which approximates the three-loop polarization operator for all Euclidean momenta.

The skeleton integral in Eq. (1) remains infrared divergent even after insertion of the three-loop vacuum polarization since $I_{3e}(0)\neq 0$. This linear infrared divergence is effectively cut off at the characteristic atomic scale $mZ\alpha$ if we restore finite virtualities of the external electron lines. As was already mentioned in the Introduction, such infrared divergence lowers the power of the factor $Z\alpha$, and respective would-be-divergent contribution turns out to be of order $\alpha^3(Z\alpha)^4$. This correction was calculated in Ref. [10], and we will not discuss it here. We carry out the subtraction of the leading low-frequency asymptote of the polarization operator insertion, which corresponds to the subtraction of the leading low-frequency asymptote in the integrand for the contribution to the energy shift $\widetilde{I}_{3e}(k)\equiv I_{3e}(k)-I_{3e}(0)$, and insert the subtracted expression in the formula for the Lamb shift in Eq. (1). We also insert an additional factor 2 in order to take into account possible insertions of the polarization operator in both photon lines. Then the contribution to the energy shift has the form

$$\delta E^{(3)}_{L}=-\frac{32\alpha^3(Z\alpha)^5}{\pi^4n^3}\left(\frac{m_r}{m}\right)^3 m\int_0^\infty\frac{dk}{k^2}\widetilde{I}_{3e}. \tag{18}$$

Calculating the integral numerically we obtain

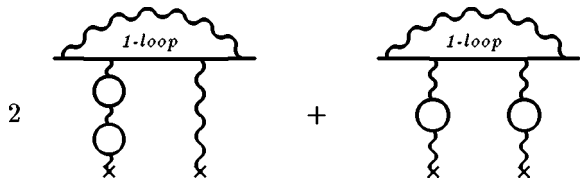


FIG. 5. One-loop electron factor and two one-loop polarizations.

$$\delta E^{(3)}_{L}=\ \ 1.015\,88(5)\,\frac{\alpha^3(Z\alpha)^5}{\pi^2n^3}\left(\frac{m_r}{m}\right)^3 m \tag{19}$$

or

$$\delta E^{(3)}_{L}=0.102\,10\ \ \mathrm{kHz} \tag{20}$$

for the $1S$ level in hydrogen.

#### *2. Hyperfine splitting*

In the case of hyperfine splitting there is no problem of infrared divergence for the radiative correction generated by the three-loop polarization insertions in Fig. 4. This correction is given by the integral

$$\delta E^{(3)}_{HFS}=\frac{16\alpha^3(Z\alpha)}{\pi^4n^3}E_F\int_0^\infty dkI_{3e}, \tag{21}$$

which arises after insertion of the doubled three-loop polarization operator in the skeleton integral in Eq. (2).

After numerical calculations we obtain

$$\delta E^{(3)}_{HFS}=1.647\,9(5)\frac{\alpha^3(Z\alpha)}{\pi^2}E_F \tag{22}$$

or

$$\delta E^{(3)}_{HFS}=0.002\,11\ \ \mathrm{kHz} \tag{23}$$

for the ground state in muonium.

### D. Diagrams with one-loop electron factor and two one-loop electron vacuum polarizations

#### *1. Lamb shift*

An analytic expression for the correction of order $\alpha^3(Z\alpha)^5$ generated by the gauge invariant set of diagrams in Fig. 5 can be obtained from the skeleton integral in Eq. (1) in the same way as the other corrections above. But this approach requires the knowledge of a new element, namely, the gauge invariant electron factor $L_L(k)$ in Fig. 6 which describes all possible insertions of the radiative photon in the electron line with two external photons. An explicit expression for the electron factor was obtained in different forms in Refs. [11–14] (we use the expression from Ref. [14])

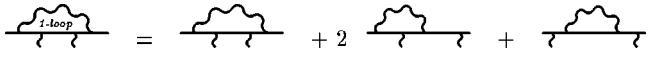


FIG. 6. One-loop electron factor.

$$L_L(k)=-\frac{1}{4}+\frac{1}{2}\ln k^2+\frac{1}{8}\frac{k^2}{1-k^2}\ln k^2$$
$$-\frac{\sqrt{k^2+4}}{2k}\ln\frac{\sqrt{k^2+4}+k}{\sqrt{k^2+4}-k}+\frac{1}{k\sqrt{k^2+4}}\ln\frac{\sqrt{k^2+4}+k}{\sqrt{k^2+4}-k}$$
$$-3\left[\frac{1}{k^2}-\frac{\sqrt{k^2+4}}{2k^3}\ln\frac{\sqrt{k^2+4}+k}{\sqrt{k^2+4}-k}\right]+\frac{k}{8}\Phi(k)$$
$$+\frac{1}{2k}\Phi(k)-\frac{2}{k^2}\left[\frac{1}{k}\Phi(k)+\ln k^2-1\right], \tag{24}$$

where

$$\Phi(k)=k\int_0^1\frac{dz}{1-k^2z^2}\ln\frac{1+k^2z(1-z)}{k^2z}. \tag{25}$$

Inserting in the skeleton integral in Eq. (1) the electron factor $(\alpha/\pi)k^2L_L(k)$, one-loop polarization operator squared, and the multiplicity factor 3 we obtain the radiative correction in the form

$$\delta E_L^{(4)}=-\frac{48\alpha^3(Z\alpha)^5}{\pi^4n^3}\left(\frac{m_r}{m}\right)^3m\int_0^\infty dk k^2L_L(k)I_{1e}^2. \tag{26}$$

It is easy to check explicitly that this integral is both ultraviolet and infrared finite. The infrared finiteness nicely correlates with the physical understanding that for the diagrams in Fig. 5 there is no correction of lower order $\alpha^2(Z\alpha)^4$ generated at the atomic scale.

After numerical calculations we obtain

$$\delta E_L^{(4)}=0.0773(4)\frac{\alpha^3(Z\alpha)^5}{\pi^2n^3}\left(\frac{m_r}{m}\right)^3m \tag{27}$$

or

$$\delta E_L^{(4)}=0.007\,77(4)\ \ \text{kHz} \tag{28}$$

for the $1S$ level in hydrogen.

#### *2. Hyperfine splitting*

We calculate the contribution to hyperfine splitting generated by the diagrams in Fig. 5 using an explicit expression for the electron factor like in the case of the Lamb shift above. This is a different electron factor which corresponds to a different spin projection. It was obtained in Ref. [15] and has the form

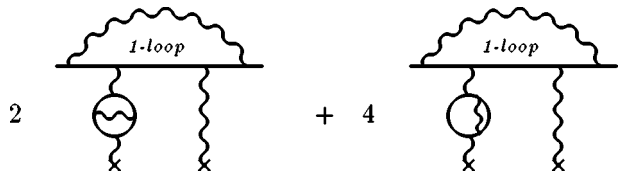


FIG. 7. One-loop electron factor and two-loop polarization.

$$L_{HFS}(k)=-\frac{3}{k^2}-\frac{4}{k^2}\ln k^2-\frac{1}{4}\frac{\ln k^2}{1-k^2}$$
$$+\frac{1}{2}\left[\ln k^2-\frac{\sqrt{k^2+4}}{k}\ln\frac{\sqrt{k^2+4}+k}{\sqrt{k^2+4}-k}\right]$$
$$+\frac{9}{2}\frac{\sqrt{k^2+4}}{k^3}\ln\frac{\sqrt{k^2+4}+k}{\sqrt{k^2+4}-k}$$
$$-\frac{4}{k^3\sqrt{k^2+4}}\ln\frac{\sqrt{k^2+4}+k}{\sqrt{k^2+4}-k}+\frac{1}{4k}\Phi(k)-\frac{4}{k^3}\Phi(k). \tag{29}$$

Inserting the electron factor $(\alpha/\pi)k^2L_{HFS}(k)$ together with the one-loop polarization operator squared and the multiplicity factor 3 in the skeleton integral in Eq. (2), we obtain the radiative correction in the form

$$\delta E_{HFS}^{(4)}=\frac{24\alpha^3(Z\alpha)}{\pi^4n^3}E_F\int_0^\infty dk k^4L_{HFS}(k)I_{1e}^2. \tag{30}$$

After numerical calculations we obtain

$$\delta E_{HFS}^{(4)}=-3.487\,2(2)\frac{\alpha^3(Z\alpha)}{\pi^2}E_F \tag{31}$$

or

$$\delta E_{HFS}^{(4)}=-0.004\,47\ \ \text{kHz} \tag{32}$$

for the ground state in muonium.

### E. Diagrams with one-loop electron factor and two-loop electron vacuum polarization

#### *1. Lamb shift*

An integral representation for the correction generated by the diagrams in Fig. 7 is obtained from the skeleton integral in Eq. (1) in the standard way

$$\delta E_L^{(5)}=-\frac{32\alpha^3(Z\alpha)^5}{\pi^4n^3}\left(\frac{m_r}{m}\right)^3m\int_0^\infty dk L_L(k)I_{2e}. \tag{33}$$

Calculating this integral numerically we obtain

$$\delta E_L^{(5)}=2.191\,3(4)\frac{\alpha^3(Z\alpha)^5}{\pi^2n^3}\left(\frac{m_r}{m}\right)^3m, \tag{34}$$

or

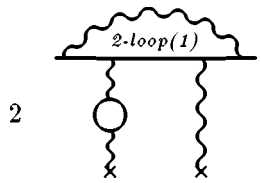


FIG. 8. One-loop polarization insertions in the electron factor and external photon.

$$\delta E_L^{(5)} = 0.220\,24(4)\ \text{kHz} \tag{35}$$

for the $1S$ level in hydrogen.

#### *2. Hyperfine splitting*

We obtain the radiative correction to hyperfine splitting generated by the diagrams in Fig. 7 inserting the electron factor $(\alpha/\pi)k^2 L_{HFS}(k)$ together with the two-loop polarization operator and the multiplicity factor 2 in the skeleton integral in Eq. (2),

$$\delta E_{HFS}^{(5)} = \frac{16\alpha^3(Z\alpha)}{\pi^4 n^3} E_F \int_0^\infty dk k^2 L_{HFS}(k) I_{2e}. \tag{36}$$

After numerical calculations we obtain

$$\delta E_{HFS}^{(5)} = -4.680\,9(1)\frac{\alpha^3(Z\alpha)}{\pi^2} E_F \tag{37}$$

or

$$\delta E_{HFS}^{(5)} = -0.006\,00\ \text{kHz} \tag{38}$$

for the ground state in muonium.

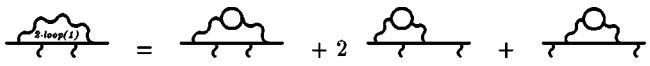


FIG. 9. One-loop polarization insertions in the electron factor.

### F. Diagrams with one-loop polarization insertions in the electron factor and in the external photon

#### *1. Lamb shift*

The contribution to the Lamb shift generated by the diagrams in Fig. 8 is similar to the contribution in Eq. (33), the only difference is that now we consider a radiatively corrected electron factor in Fig. 9 and a one-loop polarization insertion in the external photon. Insertions in the skeleton integral in Eq. (1) lead to the expression

$$\delta E_L^{(6)} = -\frac{32\alpha^3(Z\alpha)^5}{\pi^4 n^3}\left(\frac{m_r}{m}\right)^3 m \int_0^\infty dk L_L^{(2,1)}(k) I_{1e}, \tag{39}$$

where the parametric representation for the electron factor with one-loop polarization insertion in Fig. 9 has the form [13]

$$L_L^{(2,1)}(k) = \int_0^1 dv \frac{v^2(1-v^2/3)}{1-v^2} L_L(k,\lambda), \tag{40}$$

where $\lambda^2 = 4/(1-v^2)$, and $L_L(k,\lambda)$ is the one-loop electron factor in Fig. 6 for a massive photon with mass $\lambda$. An explicit representation for this electron factor was obtained in Ref. [13],

$$\begin{aligned} L_L(k,\lambda) = {} & \frac{1}{k^4}\int_0^1 dx(1+x)\left[\ln\left(1+\frac{k^2x(1-x)}{d(x,\lambda)}\right) - \frac{k^2x(1-x)}{d(x,\lambda)}\right] - \frac{1}{4k^2}\int_0^1 dx(3x-1)\ln\left(1+\frac{k^2x(1-x)}{d(x,\lambda)}\right) \\ & - \int_0^1 dx\int_0^x dy\left\{\frac{2y(x-y)+1-x}{2d(x,\lambda)} + \frac{1}{k^2}\ln\left(1+\frac{k^2y(1-y)}{d(x,\lambda)}\right) - \frac{y(1-y)}{2d(x,\lambda)a^2(x,y,\lambda)}\{k^2[2y(x-y)+1-x] \right. \\ & \left. -(2x^2+4x-4)\}\right\} - \frac{3}{4}\int_0^1 dx\int_0^x dy(x-y)\left\{\frac{k^2}{a^4(x,y,\lambda)}\left[x\left(y^2-\frac{2}{3}y\right) - \frac{1}{3}y^2 - \frac{2}{3}y\right]\right. \\ & \left. + \frac{1}{a^4(x,y,\lambda)}\left(\frac{1}{3}x^3+x^2-2x+\frac{4}{3}\right) - \frac{1-x}{a^2(x,y,\lambda)}\right\}, \end{aligned} \tag{41}$$

where

$$\begin{aligned} d(x,\lambda) &= x^2+\lambda^2(1-x), \\ a^2(x,y,\lambda) &= d(x,\lambda)+k^2y(1-y). \end{aligned} \tag{42}$$

Calculating the integral in Eq. (39) numerically we obtain

$$\delta E_L^{(6)} = 0.037\,36(1)\frac{\alpha^3(Z\alpha)^5}{\pi^2 n^3}\left(\frac{m_r}{m}\right)^3 m \tag{43}$$

or

$$\delta E_L^{(6)} = 0.003\,75\ \text{kHz} \tag{44}$$

for the $1S$ level in hydrogen.

#### *2. Hyperfine splitting*

We obtain the radiative correction to hyperfine splitting generated by the diagrams in Fig. 8 inserting the radiatively corrected electron factor $(\alpha/\pi)k^2L^{(2,1)}_{HFS}(k)$ in Fig. 9 together with the one-loop polarization operator and the multiplicity factor 2 in the skeleton integral in Eq. (2),

$$\delta E^{(6)}_{HFS}=\frac{16\alpha^3(Z\alpha)}{\pi^4 n^3}E_F\int_0^\infty dk k^2 L^{(2,1)}_{HFS}(k)I_{1e}. \qquad (45)$$

The parametric representation for the electron factor $L^{(2,1)}_{HFS}(k)$ has the form [16]

$$L^{(2,1)}_{HFS}(k)=\int_0^1 dv\frac{v^2(1-v^2/3)}{1-v^2}L_{HFS}(k,\lambda), \qquad (46)$$

where $\lambda^2=4/(1-v^2)$, and $L_{HFS}(k,\lambda)$ is the one-loop electron factor in Fig. 6 for a massive photon with mass $\lambda$. An explicit representation for this electron factor was obtained in Ref. [16]

$$L_{HFS}(k,\lambda)=\frac{1}{2}\int_0^1 dx\int_0^x dy\left(\frac{A(\lambda;x,y)}{k^2y(1-y)+x^2+\lambda^2(1-x)}-\frac{k^2B(\lambda;x,y)}{[k^2y(1-y)+x^2+\lambda^2(1-x)]^2}\right), \qquad (47)$$

where

$$A(\lambda;x,y)=a_0(x,y)+a_1(x,y)\frac{\lambda^2(1-x)}{x^2+\lambda^2(1-x)}, \qquad (48)$$

$$B(\lambda;x,y)=b_0(x,y)+b_1(x,y)\frac{\lambda^2(1-x)}{x^2+\lambda^2(1-x)}+b_2(x,y)\times\left(\frac{\lambda^2(1-x)}{x^2+\lambda^2(1-x)}\right)^2, \qquad (49)$$

and

$$a_0(x,y)=(1-x)^2-x-2\frac{1-x}{x}+\frac{2}{x}\left(1-\frac{2}{x}\right)y^2, \qquad (50)$$

$$a_1(x,y)=\left(\frac{2}{x}-3(1-x)\right)y+\left(\frac{4}{x^2}-\frac{2}{x}-2\right)y^2, \qquad (51)$$

$$b_0(x,y)=x\left(1-\frac{x}{2}\right)y+\left(-\frac{4}{x}+1+x\right)y^2+\left(\frac{6}{x^2}-\frac{4}{x}-3\right)y^3+\frac{2}{x}y^4, \qquad (52)$$

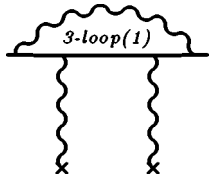


FIG. 10. One-loop polarization insertions in the electron factor.

$$b_1(x,y)=\left(\frac{4}{x}-1-2x+\frac{x^2}{2}\right)y^2+\left(-\frac{10}{x^2}+\frac{8}{x}+4-2x\right)y^3+\left(1-\frac{2}{x}\right)y^4, \qquad (53)$$

$$b_2(x,y)=\frac{4-x^2}{x^2}(1-x)y^3. \qquad (54)$$

After numerical calculations we obtain

$$\delta E^{(6)}_{HFS}=-0.533\,3(5)\frac{\alpha^3(Z\alpha)}{\pi^2}E_F \qquad (55)$$

or

$$\delta E^{(6)}_{HFS}=-0.000\,68\ \text{kHz} \qquad (56)$$

for the ground state in muonium.

### G. Diagrams with two one-loop polarization insertions in the electron factor

#### *1. Lamb shift*

The contribution to the Lamb shift generated by the diagrams in Fig. 10 is similar to the correction generated by the one-loop polarization insertion in the electron factor calculated in Ref. [13]. The explicit expression for this correction

$$\delta E^{(7)}_L=-\frac{16\alpha^3(Z\alpha)^5}{\pi^4 n^3}\left(\frac{m_r}{m}\right)^3 m\int_0^\infty dk\frac{L^{(3,1)}_L(k)-L^{(3,1)}_L(0)}{k^2} \qquad (57)$$

differs from the respective expression in Ref. [13] only due to the difference between the electron factor with one one-loop polarization insertion $L^{(2,1)}_L(k)$ in Eq. (40) (see Fig. 9) and the electron factor with two one-loop polarization insertions $L^{(3,1)}_L(k)$ in Fig. 11.

The photon line with two one-loop polarization insertions has the form

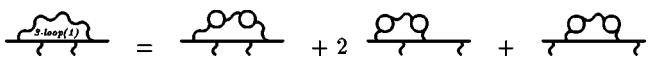


FIG. 11. Two one-loop polarization insertions in the electron factor.

$$k^2 I_1^2(k^2) = \int_0^1 dv_1 \int_0^1 dv_2 \frac{v_1^2(1-v_1^2/3)}{1-v_1^2} \frac{v_2^2(1-v_2^2/3)}{1-v_2^2} \frac{k^2}{(\lambda_1^2+k^2)(\lambda_2^2+k^2)}$$

$$= \int_0^1 dv_1 \int_0^1 dv_2 \frac{v_1^2(1-v_1^2/3)}{1-v_1^2} \frac{v_2^2(1-v_2^2/3)}{1-v_2^2} \frac{1}{\lambda_1^2-\lambda_2^2}\left[\frac{\lambda_1^2}{\lambda_1^2+k^2} - \frac{\lambda_2^2}{\lambda_2^2+k^2}\right], \tag{58}$$

where $\lambda_1^2 = 4/(1-v_1^2)$ and $\lambda_2^2 = 4/(1-v_2^2)$.

Then the electron factor with two one-loop polarization insertions in Fig. 11 can be written as

$$L_L^{(3,1)}(k) = \int_0^1 dv_1 \int_0^1 dv_2 \frac{v_1^2(1-v_1^2/3)}{1-v_1^2} \frac{v_2^2(1-v_2^2/3)}{1-v_2^2} \frac{[\lambda_1^2 L_L(k,\lambda_1) - \lambda_2^2 L_L(k,\lambda_2)]}{\lambda_1^2-\lambda_2^2}$$

$$= \int_0^1 dv \frac{v^2(1-v^2/3)}{1-v^2}\left[v\left(1-\frac{v^2}{3}\right)\ln\frac{1+v}{1-v} - \frac{16}{9} + \frac{2v^2}{3}\right] L_L(k,\lambda). \tag{59}$$

Calculating the integral for the energy shift in Eq. (57) numerically we obtain

$$\delta E_L^{(7)} = -0.012\,610(3)\frac{\alpha^3(Z\alpha)^5}{\pi^2 n^3}\left(\frac{m_r}{m}\right)^3 m \tag{60}$$

or

$$\delta E_L^{(7)} = -0.001\,27 \ \text{kHz} \tag{61}$$

for the $1S$ level in hydrogen.

#### *2. Hyperfine splitting*

The contribution to hyperfine splitting generated by the diagrams in Fig. 10 is similar to the correction generated by the one-loop polarization insertion in the electron factor which was calculated in Ref. [16]. The explicit expression for this correction has the form

$$\delta E_{HFS}^{(7)} = \frac{8\alpha^3(Z\alpha)}{\pi^4 n^3} E_F \int_0^\infty dk L_{HFS}^{(3,1)}(k), \tag{62}$$

where [compare Eq. (59)]

$$L_{HFS}^{(3,1)}(k) = \int_0^1 dv \frac{v^2(1-v^2/3)}{1-v^2}\left[v\left(1-\frac{v^2}{3}\right)\ln\frac{1+v}{1-v} - \frac{16}{9} + \frac{2v^2}{3}\right] L_{HFS}(k,\lambda). \tag{63}$$

After numerical calculations we obtain

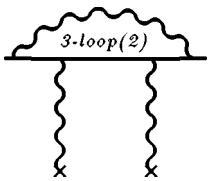


FIG. 12. Two-loop polarization insertions in the electron factor.

$$\delta E_{HFS}^{(7)} = -0.309\,05(7)\frac{\alpha^3(Z\alpha)}{\pi^2} E_F \tag{64}$$

or

$$\delta E_{HFS}^{(7)} = -0.000\,40 \ \text{kHz} \tag{65}$$

for the ground state in muonium.

### H. Diagrams with two-loop polarization insertion in the electron factor

#### *1. Lamb shift*

The contribution to the Lamb shift generated by the diagrams in Fig. 12 is similar to the correction generated by the one-loop polarization insertion in the electron factor which was calculated in Ref. [13]. The explicit expression for this correction

$$\delta E_L^{(8)} = -\frac{16\alpha^3(Z\alpha)^5}{\pi^4 n^3}\left(\frac{m_r}{m}\right)^3 m \int_0^\infty dk \frac{L_L^{(3,2)}(k) - L_L^{(3,2)}(0)}{k^2}, \tag{66}$$

differs from the respective expression in Ref. [13] only due to the difference between the electron factor with one-loop polarization insertion $L_L^{(2,1)}(k)$ in Eq. (40) (see Fig. 9) and the electron factor with the two-loop polarization insertion $L_L^{(3,2)}(k)$ in Fig. 13,

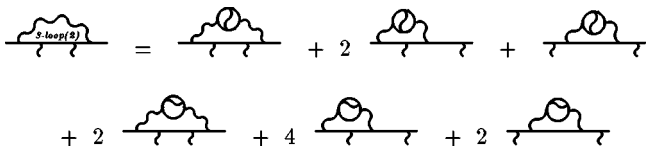


FIG. 13. Two-loop polarization insertions in the electron factor.

$$L_L^{(3,2)}(k)=\frac{2}{3}\int_0^1\frac{v\,dv}{1-v^2}\Bigg\{(3-v^2)(1+v^2)\Bigg[\mathrm{Li}_2\left(-\frac{1-v}{1+v}\right)+2\ \mathrm{Li}_2\left(\frac{1-v}{1+v}\right)+\frac{3}{2}\ln\frac{1+v}{1-v}\ln\frac{1+v}{2}-\ln\frac{1+v}{1-v}\ln v\Bigg]+\left[\frac{11}{16}(3-v^2)(1+v^2)+\frac{v^4}{4}\right]\ln\frac{1+v}{1-v}+\left[\frac{3}{2}v(3-v^2)\ln\frac{1-v^2}{4}-2v(3-v^2)\ln v\right]+\frac{3}{8}v(5-3v^2)\Bigg\}L_L(k,\lambda), \tag{67}$$

where $\lambda^2=4/(1-v^2)$, and the electron factor with a massive photon $L_L(k,\lambda)$ is written explicitly in Eq. (41).

A convenient expression for the subtracted massive electron factor $L_L(k,\lambda)-L_L(0,\lambda)$ was obtained in Ref. [13], and using those old formulas we immediately obtain

$$\delta E_L^{(8)}=-0.245\,71(7)\,\frac{\alpha^3(Z\alpha)^5}{\pi^2 n^3}\left(\frac{m_r}{m}\right)^3 m \tag{68}$$

or

$$\delta E_L^{(8)}=-0.024\,70\ \ \mathrm{kHz} \tag{69}$$

for the $1S$ level in hydrogen.

#### *2. Hyperfine splitting*

The contribution to hyperfine splitting generated by the diagrams in Fig. 12 is similar to the correction generated by the one-loop polarization insertion in the electron factor which was calculated in Ref. [16]. The explicit expression for this correction has the form

$$\delta E_{HFS}^{(8)}=\frac{8\alpha^3(Z\alpha)}{\pi^4 n^3}E_F\int_0^\infty dk L_{HFS}^{(3,2)}(k), \tag{70}$$

where

$$L_{HFS}^{(3,2)}(k)=\frac{2}{3}\int_0^1\frac{v\,dv}{1-v^2}\Bigg\{(3-v^2)(1+v^2)\Bigg[\mathrm{Li}_2\left(-\frac{1-v}{1+v}\right)+2\mathrm{Li}_2\left(\frac{1-v}{1+v}\right)+\frac{3}{2}\ln\frac{1+v}{1-v}\ln\frac{1+v}{2}-\ln\frac{1+v}{1-v}\ln v\Bigg]+\left[\frac{11}{16}(3-v^2)(1+v^2)+\frac{v^4}{4}\right]\ln\frac{1+v}{1-v}+\left[\frac{3}{2}v(3-v^2)\ln\frac{1-v^2}{4}-2v(3-v^2)\ln v\right]+\frac{3}{8}v(5-3v^2)\Bigg\}L_{HFS}(k,\lambda), \tag{71}$$

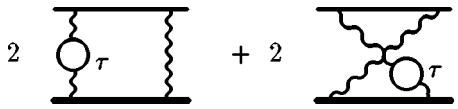


FIG. 14. $\tau$ lepton polarization contribution to hyperfine splitting.

and $L_{HFS}(k,\lambda)$ is the electron factor with a massive photon from Eq. (47).

After numerical calculations we obtain

$$\delta E_{HFS}^{(8)}=-0.123\,9(6)\frac{\alpha^3(Z\alpha)}{\pi^2}E_F \tag{72}$$

or

$$\delta E_{HFS}^{(8)}=-0.000\,16\ \ \mathrm{kHz} \tag{73}$$

for the ground state in muonium.

### III. $\tau$ POLARIZATION CONTRIBUTION

The one-loop $\tau$-lepton polarization contribution to hyperfine splitting generating the diagrams in Fig. 14 may be calculated exactly. Again the scattering approximation is sufficient for calculation of this correction (see, e.g., Ref. [17]). First time the $\tau$-lepton contribution was estimated in Ref. [18]. At that moment this correction was of purely academic interest, and a crude step-function model for the one-loop polarization spectral function was used in Ref. [18]. Due to a spectacular experimental progress during the last two decades, now we need a more accurate result for the $\tau$-lepton contribution to hyperfine splitting.

The general expression for this correction has the form (compare, e.g., Ref. [2])

$$\delta E_\tau=\frac{\alpha(Z\alpha)}{\pi^2\mu}\widetilde{E}_F\int\frac{d^4k}{i\pi^2}\frac{1}{k^2}\Bigg[\frac{1}{k^2+2m_\mu k_0}+\frac{1}{k^2-2m_\mu k_0}\Bigg]\frac{3k_0^2-2\mathbf{k}^2}{k^2-2m_e k_0}I_{1\tau}, \tag{74}$$

where

$$I_{1\tau}=\int_0^1 dv\frac{v^2(1-v^2/3)}{4m_\tau^2+k^2(1-v^2)} \tag{75}$$

is the one-loop $\tau$-lepton vacuum polarization, the dimensionless parameter $\mu$ is given by the expression $\mu=m_e/(2m_\mu)$, and the Fermi energy $\widetilde{E}_F$, unlike the expression in Eq. (3), does not include the factor $1+a_\mu$. The expression in Eq. (74) may be obtained from the integral for the skeleton graphs with two exchanged photons by the substitution $1/k^2\to 2I_{1\tau}$, where the additional factor 2 has the combinatorial origin.

After the Wick rotation, transition to the four-dimensional spherical coordinates, and to the dimensionless integration momenta measured in the units of the electron mass the expression in Eq. (74) acquires the form

$$\delta E_\tau = \frac{\alpha(Z\alpha)}{\pi^2}\frac{m_e}{m_\mu}E_F 8\int_0^\infty dk k\left[\frac{1}{\mu k}(\sqrt{1+\mu^2k^2}-\mu k) - \frac{1}{2}\left(\mu k\sqrt{1+\mu^2k^2}-\mu^2k^2-\frac{1}{2}\right)-\frac{1}{k}(\sqrt{4+k^2}-k) + \frac{1}{2}\left(\frac{k}{4}\sqrt{4+k^2}-\frac{k^2}{4}-\frac{1}{2}\right)\right]\int_0^1 dv \frac{v^2(1-v^2/3)}{\frac{4m_\tau^2}{m_e^2}+k^2(1-v^2)}$$

$$\equiv \delta\epsilon_\tau \frac{\alpha(Z\alpha)}{\pi^2}\frac{m_e}{m_\mu}E_F. \tag{76}$$

This is a finite integral which can be calculated numerically with arbitrary accuracy. Numerically we obtain

$$\delta\epsilon_\tau = 0.019\,190\,6\ldots. \tag{77}$$

One can also obtain an analytic expression for leading terms in the expansion of the $\tau$-lepton polarization contribution to the hyperfine splitting over the small parameters $m_\mu/m_\tau$, $m_e/m_\mu$, and $m_e/m_\tau$. Let us describe briefly calculation of the leading terms in this expansion. First, we write the dimensionless contribution to the energy splitting as a sum of two terms

$$\delta\epsilon_1 = 8\int_0^\infty dk k\left[\frac{1}{\mu k}(\sqrt{1+\mu^2k^2}-\mu k)-\frac{1}{2}\left(\mu k\sqrt{1+\mu^2k^2}-\mu^2k^2-\frac{1}{2}\right)\right]\int_0^1 dv\,\frac{v^2(1-v^2/3)}{\frac{4m_\tau^2}{m_e^2}+k^2(1-v^2)}, \tag{78}$$

$$\delta\epsilon_2 = 8\int_0^\infty dk k\left[-\frac{1}{k}(\sqrt{4+k^2}-k)+\frac{1}{2}\left(\frac{k}{4}\sqrt{4+k^2}-\frac{k^2}{4}-\frac{1}{2}\right)\right]\int_0^1 dv\frac{v^2(1-v^2/3)}{\frac{4m_\tau^2}{m_e^2}+k^2(1-v^2)}, \tag{79}$$

which correspond to the two first and two last terms in the square brackets in the integrand in Eq. (76), respectively. The integral $\delta\epsilon_2$ is proportional to $m_e^2/m_\tau^2$, and is too small to be of any interest for us here. The integral $\delta\epsilon_1$, as we will see, is proportional to a much larger parameter $m_\mu^2/m_\tau^2$, and gives a leading contribution to $\delta\epsilon_\tau$. To calculate it we once again rescale the integration momentum $q=\mu k$,

$$\delta\epsilon_1 = 8\int_0^\infty dq\left[(\sqrt{1+q^2}-q)-\frac{q}{2}\left(q\sqrt{1+q^2}-q^2-\frac{1}{2}\right)\right]\times\int_0^1 dv\,\frac{v^2(1-v^2/3)}{\left(\frac{m_\tau}{m_\mu}\right)^2+q^2(1-v^2)}. \tag{80}$$

To extract the leading terms in the asymptotic expansion of this integral we introduce an auxiliary parameter $\sigma$ which satisfies the inequality $1\ll\sigma\ll m_\tau/m_\mu$. We use the parameter $\sigma$ to separate the momentum integration into two regions, a region of small momenta $0\leqslant q\leqslant\sigma$, and a region of large momenta $\sigma\leqslant q<\infty$. In the region of small momenta we use the low-momentum expansion of the polarization operator and obtain

$$\delta\epsilon_1^< = 8\int_0^\sigma dq\left[(\sqrt{1+q^2}-q)-\frac{q}{2}\left(q\sqrt{1+q^2}-q^2-\frac{1}{2}\right)\right]\times\frac{4}{15}\left(\frac{m_\mu}{m_\tau}\right)^2 \approx\left(\frac{6}{5}\ln\sigma+\frac{6}{5}\ln 2+\frac{1}{2}\right)\left(\frac{m_\mu}{m_\tau}\right)^2. \tag{81}$$

In the region of large momenta $q\gg 1$ we use the large momentum expansion of the skeleton integrand and obtain

$$\delta\epsilon_1^> = \int_\sigma^\infty dq\left(\frac{9}{2q}\right)\int_0^1 dv\,\frac{v^2(1-v^2/3)}{\left(\frac{m_\tau}{m_\mu}\right)^2+q^2(1-v^2)} \approx\left(\frac{6}{5}\ln\frac{m_\tau}{m_\mu}-\frac{6}{5}\ln\sigma-\frac{6}{5}\ln 2+\frac{77}{50}\right)\left(\frac{m_\mu}{m_\tau}\right)^2. \tag{82}$$

For the intermediate momenta $q\simeq\sigma$ both approximations for the integrand are valid simultaneously, so in the sum of the low-momenta and high-momenta integrals all $\sigma$-dependent terms cancel and we obtain a $\sigma$-independent result

$$\delta\epsilon_1 = \delta\epsilon_1^< + \delta\epsilon_1^> = \left(\frac{6}{5}\ln\frac{m_\tau}{m_\mu}+\frac{51}{25}\right)\left(\frac{m_\mu}{m_\tau}\right)^2 \approx 0.019\,185. \tag{83}$$

The leading terms in the asymptotic expression for the $\tau$-lepton contribution were also estimated in Ref. [18]. We disagree with both terms obtained in Ref. [18]. However, numerically for the real parameters of the $\tau$ lepton, the difference between the result in Ref. [18] and in Eq. (83) is only about $4\times10^{-3}$.

Comparing the approximate result in Eq. (83) with the result of the numerical calculation of the integral in Eq. (76), we see that their difference is about $5\times10^{-6}$. Due to overall smallness of the correction under consideration, this means that the analytic expression in Eq. (83) is sufficient for all phenomenological purposes.

Finally, the $\tau$ polarization contribution to the hyperfine splitting may be approximated by the expression

$$\delta E_\tau = \delta\epsilon_\tau\frac{\alpha(Z\alpha)}{\pi^2}\frac{m_e}{m_\mu}E_F \approx\left(\frac{6}{5}\ln\frac{m_\tau}{m_\mu}+\frac{51}{25}\right)\frac{\alpha(Z\alpha)}{\pi^2}\frac{m_e m_\mu}{m_\tau^2}E_F, \tag{84}$$

or numerically

$$\delta E_\tau = 0.002\,2\ \ \text{kHz} \tag{85}$$

for the ground state in muonium.

## IV. DISCUSSION OF RESULTS

In this paper we calculated a series of nonrecoil corrections of order $\alpha^3(Z\alpha)^5 m$ to the Lamb shift, and a series of nonrecoil corrections of order $\alpha^3(Z\alpha)E_F$ to hyperfine splitting generated by the diagrams in Figs. 2, 3, 4, 5, 7, 8, 10, and 12. Collecting all contributions to the Lamb shift in Eq. (6), Eq. (13), Eq. (18), Eq. (27), Eq. (34), Eq. (43), Eq. (60), and Eq. (68) we obtain

$$\delta E_L^{tot} = 2.6519(6)\frac{\alpha^3(Z\alpha)^5}{\pi^2 n^3}\left(\frac{m_r}{m}\right)^3 m \tag{86}$$

or

$$\delta E_L^{tot} = 0.266\,53(6)\ \ \mathrm{kHz} \tag{87}$$

for the $1S$ level in hydrogen.

Collecting all contributions to hyperfine splitting in Eq. (9), Eq. (16), Eq. (21), Eq. (31), Eq. (36), Eq. (55), Eq. (64), and Eq. (72) we obtain

$$\delta E_{HFS}^{tot} = -1.358(1)\frac{\alpha^3(Z\alpha)}{\pi^2}E_F \tag{88}$$

or

$$\delta E_{HFS}^{tot} = -0.001\,74\ \ \mathrm{kHz} \tag{89}$$

for the ground state in muonium.

Both the corrections to the Lamb shift and hyperfine could be easily estimated before the actual calculation is carried out. They are suppressed by an additional factor $\alpha/\pi$ in comparison with the corrections of the lower order in $\alpha$. In the case of the Lamb shift this means that corrections of order $\alpha^3(Z\alpha)^5 m$ should be as large as 1 kHz for the $1S$ level in hydrogen. Corrections of this magnitude are phenomenologically relevant at the current level of experimental and theoretical accuracy (see, e.g., Ref. [1]). We expect that the largest contribution will be generated by the gauge invariant set of diagrams with insertions of three radiative photons in the electron line in the skeleton diagrams in Fig. 1. Work on calculation of the contribution of these diagrams as well as of all other remaining corrections of order $\alpha^3(Z\alpha)^5 m$ to the Lamb shift, and corrections of order $\alpha^3(Z\alpha)E_F$ to hyperfine splitting, is now in progress, and we hope to report on its results in the near future.

We also obtained above the $\tau$ lepton polarization contribution to the hyperfine splitting

$$\delta E_\tau = \left(\frac{6}{5}\ln\frac{m_\tau}{m_\mu} + \frac{51}{25}\right)\frac{\alpha(Z\alpha)}{\pi^2}\,\frac{m_e m_\mu}{m_\tau^2}E_F, \tag{90}$$

which numerically gives

$$\delta E_\tau = 0.0022\ \ \mathrm{kHz} \tag{91}$$

for the ground state in muonium.

The magnitude of this contribution is comparable to a number of other new corrections, obtained recently, for example, to some nonlogarithmic three-loop radiative-recoil corrections [19], and to the contributions due the two-loop hadron polarizations in Ref. [20].

## ACKNOWLEDGMENTS

This work was supported by the NSF, Grant No. PHY-0138210. The work of V. A. Shelyuto was also supported in part by the RFBR, Grant No. 03-02-16843.

[1] M.I. Eides, H. Grotch, and V.A. Shelyuto, Phys. Rep. **342**, 63 (2001).
[2] M.I. Eides, S.G. Karshenboim, and V.A. Shelyuto, Ann. Phys. (N.Y.) **205**, 231 (1991).
[3] G. Kallen and A. Sabry, K. Dan. Vidensk. Selsk. Mat. Fys. Medd. **29**, 17 (1955).
[4] J. Schwinger, *Particles, Sources and Fields* (Addison-Wesley, Reading, MA, 1973), Vol. 2.
[5] P.A. Baikov and D.J. Broadhurst, e-print hep-ph/9504398.
[6] P.A. Baikov, Phys. Lett. B **385**, 404 (1996).
[7] K.G. Chetyrkin, J.H. Kühn, and M. Steinhauser, Nucl. Phys. B **482**, 213 (1996); **505**, 40 (1997).
[8] K.G. Chetyrkin, R. Harlander, J.H. Kühn, and M. Steinhauser, Nucl. Instrum. Methods Phys. Res. A **389**, 354 (1997).
[9] K.G. Chetyrkin, R. Harlander, J.H. Kühn, and M. Steinhauser, Nucl. Phys. B **503**, 354 (1997).
[10] M.I. Eides and H. Grotch, Phys. Rev. A **52**, 3360 (1995).
[11] G. Bhatt and H. Grotch, Ann. Phys. (N.Y.) **178**, 1 (1987).
[12] M.I. Eides and H. Grotch, Phys. Lett. B **301**, 127 (1993).
[13] M.I. Eides and H. Grotch, Phys. Lett. B **308**, 389 (1993).
[14] M.I. Eides, H. Grotch, and V.A. Shelyuto, Phys. Rev. A **55**, 2447 (1997).
[15] M.I. Eides, S.G. Karshenboim, and V.A. Shelyuto, Phys. Lett. B **229**, 285 (1989); Pis'ma Zh. Éksp. Teor. Fiz. **50**, 3 (1989) [JETP Lett. **50**, 1 (1989)]; Yad. Fiz. **50**, 1636 (1989) [Sov. J. Nucl. Phys. **50**, 1015 (1989)].
[16] M.I. Eides, S.G. Karshenboim, and V.A. Shelyuto, Phys. Lett. B **249**, 519 (1990).
[17] M.I. Eides, H. Grotch, and V.A. Shelyuto, Phys. Rev. D **67**, 113003 (2003).
[18] J.R. Sapirstein, E.A. Terray, and D.R. Yennie, Phys. Rev. Lett. **51**, 982 (1983); Phys. Rev. D **29**, 2290 (1984).
[19] M.I. Eides, H. Grotch, and V.A. Shelyuto, Phys. Rev. D **65**, 013003 (2002).
[20] S.I. Eidelman, S.G. Karshenboim, and V.A. Shelyuto, Can. J. Phys. **80**, 1297 (2002).